BASIC SCIENCE

Orexin Plays a Role in Growth Impediment Induced by Obstructive Sleep Breathing in Rats

Ariel Tarasiuk, PhD[1,2,3]; Avishag Levi, MsC[1,3]; Mohammad H. Assadi, MsC[1,3]; Ariel Troib, MsC[1]; Yael Segev, PhD[1]

[1]Shraga Segal Department of Microbiology and Immunology, Ben-Gurion University of the Negev, Beer-Sheva, Israel; [2]Sleep-Wake Disorders Unit, Soroka University Medical Center, Beer-Sheva, Israel; [3]Department of Physiology, Faculty of Health Sciences, Ben-Gurion University of the Negev, Beer-Sheva, Israel

Study Objectives: The mechanisms linking sleep disordered breathing with impairment of sleep and bone metabolism/architecture are poorly understood. Here, we explored the role of the neuropeptide orexin, a respiratory homeostasis modulator, in growth retardation induced in an upper airway obstructed (AO) rat model.

Methods: The tracheae of 22-day-old rats were narrowed; AO and sham-control animals were monitored for 5 to 7 w. Growth parameters, food intake, sleep/wake activity, and serum hormones were measured. After euthanasia, growth plate (GP) histology, morphometry, orexin receptors (OXR), and related mediators were analyzed. The effect of dual orexin receptor antagonist (almorexant 300 mg/kg) on sleep and GP histology were also investigated.

Results: The AO group slept 32% less; the time spent in slow wave and paradoxical sleep during light period and slow wave activity was reduced. The AO group gained 46% less body weight compared to the control group, despite elevated food intake; plasma ghrelin increased by 275% and leptin level decreased by 44%. The impediment of bone elongation and bone mass was followed by a 200% increase in OX1R and 38% reduction of local GP ghrelin proteins and growth hormone secretagogue receptor 1a. Sry-related transcription factor nine (Sox9), a molecule mediating cartilage ossification, was downregulated and the level of transcription factor peroxisome proliferator-activated receptor gamma was upregulated, explaining the bone architecture abnormalities. Administration of almorexant restored sleep and improved GP width in AO animals.

Conclusions: In AO animals, enhanced expression of orexin and OX1R plays a role in respiratory induced sleep and growth abnormalities.

Keywords: growth, orexin, rat, sleep, upper airway loading

Citation: Tarasiuk A, Levi A, Assadi MH, Troib A, Segev Y. Orexin plays a role in growth impediment induced by obstructive sleep breathing in rats. *SLEEP* 2016;39(4):887–897.

Significance

Children with sleep disordered breathing often exhibit abnormal growth; the juvenile rat upper airway obstruction model mimics many of the features of the human disorder including growth retardation. The mechanisms linking upper airway obstruction - induced sleep, energy metabolism abnormalities, and bone metabolism/architecture impairment are poorly understood. This study explored the effects of surgical tracheal narrowing on growth plate metabolism pathways in growing animals. Here, we show for the first time that the local growth plate shift in orexin and ghrelin play a role in bone metabolism/architecture, abnormal sleep and energy metabolism. These findings indicate that orexin and ghrelin may have potential clinical relevance in growth and sleep impairment in pediatric sleep disordered breathing.

INTRODUCTION

Chronic upper airway obstruction (AO) in animal models, similar to human sleep disordered breathing (SDB), elicits endocrine derangements leading to growth retardation in juveniles[1–6] and bone mass loss in adults.[7] Children with SDB often exhibit abnormal growth, and the juvenile AO rat model mimics many of the features of the human disorder including growth retardation.[4–6,8] The mechanisms linking AO-induced sleep, energy metabolism abnormalities, and bone metabolism/architecture impairment are poorly understood.

Sleep homeostasis plays an important role in normal growth; AO in children and animals is associated with abnormal sleep and reduced growth hormone/insulin-like growth factor 1 (GH/IGF-1) axis, leading to growth retardation.[3,9,10] However, in AO animals stimulation of the GH axis with ritanserin only partially restored growth.[5,6] This finding indicates that other pathways are involved in sleep abnormalities associated with this growth retardation. Seeking the identity of these pathways, we focused our attention on orexin and ghrelin peptides in AO animals. Orexins are neuropeptides that have a key role in regulation of sleep, ventilation, and orexigenic control.[11–16] Orexin regulates brain states and adaptive behaviors; both arousal and breathing centers receive stimulatory inputs from orexinergic neurons. During AO the respiratory system undergoes adaptive changes in order to maintain proper ventilation and enhanced hypothalamic orexin is involved in this response,[6,8] most likely by affecting carbon dioxide chemoreception.[16] Most recently, orexin acting peripherally through orexin receptor 1 (OX1R) has been implicated in regulation of bone metabolism/architecture by affecting growth plate (GP) ghrelin levels.[15] Several signaling pathways of ghrelin, including phosphatidylinositol 3-kinase (PI3K)/AKT, were found to play a role in chondrogenesis and bone development.[17,18] Orexins stimulate lipogenesis via increased transcription factor peroxisome proliferator-activated receptor gamma (PPARγ) and the PI3K/AKT pathway in marrow adipose tissue, which can cause bone mass loss and increased marrow adipogenesis.[19–24]

Linear growth occurs at the end of long bones in the GP by a process of endochondral ossification[25–27] (Figure S1, supplemental material). Endochondral ossification is a tightly regulated process whereby cartilage anlagen grows through chondrocyte proliferation and hypertrophy; subsequently, cartilage is replaced by bone. Endocrine or paracrine stimuli cause extensive proliferation of resting chondrocytes. The proliferating chondrocytes express specific markers such as collagen type II and aggrecan, whose production is regulated by chondrogenic factor Sry-related transcription factor nine (Sox9).[28] At the end of proliferation, chondrocytes begin to differentiate into type X collagen, producing hypertrophic

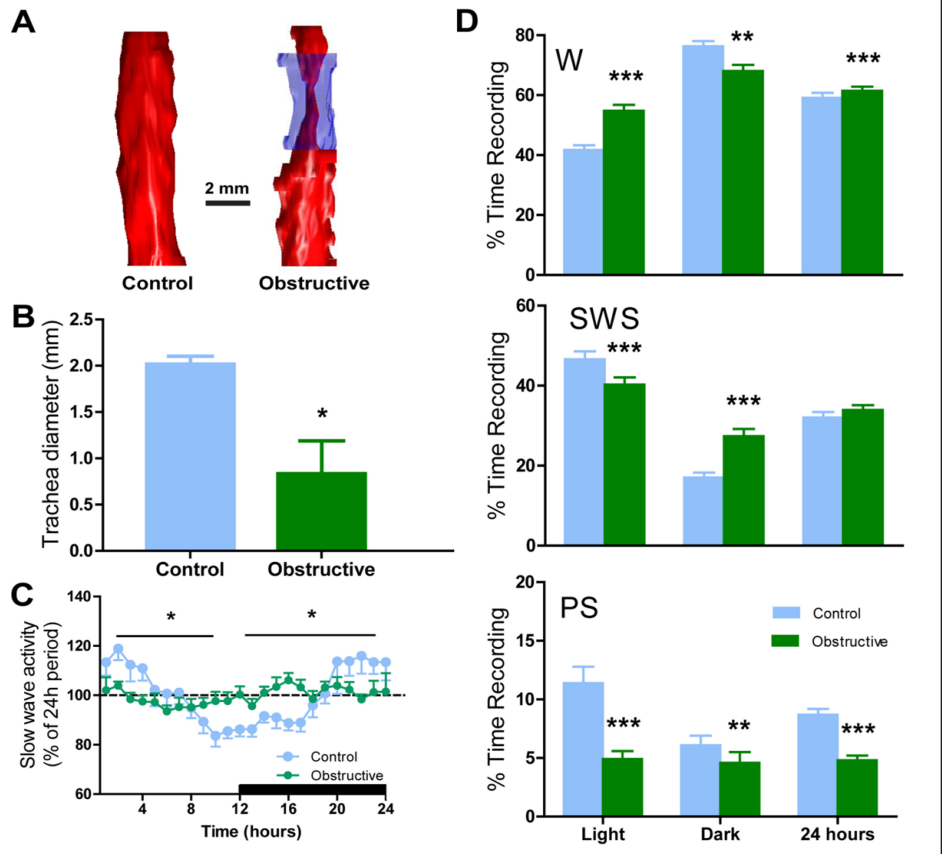

Figure 1—Effect of upper airway obstruction on sleep. **(A)** Trachea three-dimensional (3D) magnetic resonance imaging; **(B)** Trachea diameter (n = 7 in each group); **(C)** Hourly average of electroencephalogram normalized slow wave activity (n = 10 controls and n = 8 airway obstructed [AO]). Black horizontal bars represent the light-off (active) period on a 12:12-h cycle. **(D)** Spontaneous sleep during 12-h lights-on period (Light), 12-h dark period (Dark), and the whole day (n = 12 controls and n = 11 AO); W, wake; SWS, slow wave sleep; PS, paradoxical sleep; *P < 0.05 **(B)** unpaired two-tailed *t* test; *P < 0.01, **P < 0.005, ***P < 0.001 indicates statistical difference between groups (C,D) by two-way analysis of variance followed by Student-Newman-Keuls test **(C)**.

chondrocytes. Chondrocyte maturation is mediated by several factors including vascular endothelial growth factor, matrix metalloproteinase 13 (MMP-13), and receptor activator of nuclear factor kappa-B Ligand (RANKL). MMP-13 targets cartilage degradation,[29] a process locally regulated by IGF-1[16,30] and runt-related transcription factor 2.[31]

Using a juvenile rat model we explored the involvement of orexin in GP metabolism/architecture abnormalities induced by sleep breathing disorder. We hypothesize that upregulation of orexin leads to abnormal bone architecture/metabolism in AO animals. We found that enhanced expression of orexin was associated with AO-induced sleep and growth abnormalities, probably by altering orexin-ghrelin balance.

METHODS

Animals

Male Sprague-Dawley 22-day-old rats (53–55 g) were used. Animals were kept on 12-12 light-dark cycle with lights on 13:00 at 23 ± 1.0°C. Food and water were given *ad libitum*. This study was approved by the Ben-Gurion University of the Negev Animal Use and Care Committee protocol number: IL-23-04-2012, and complied with the American Physiological Society Guidelines.

Surgery

The technique used for sham surgery and to induce AO in 22-day-old male rats (day 0) was as previously described.[4–6,8,32–36] Animals were anesthetized with tribromoethanol (200 mg/kg) administered intraperitoneally. A midline ventral cervical incision was made, and the trachea exposed and dissected so as not to damage adjacent structures. A circumferential silicon band 0.5 cm long was placed around the trachea to induce tracheal narrowing (Figure 1A). Controls underwent sham surgery with no tracheal narrowing. On day 38 after AO/sham surgery a telemetric transmitter (TL11M2-F20-EET Data Sciences International, DSI, St. Paul, MN, USA) was implanted, enabling recording of electroencephalography (EEG) and dorsal neck electromyography (EMG) as previously described.[6,8] An arterial catheter was implanted in the left carotid artery for sampling of arterial blood in unrestrained animals.[37,38] A 3F heparin-coated PU catheter (CBAS-C30, Solomon Scientific, San Antonio, TX, USA) was inserted into the common carotid artery, ensuring that the catheter tip was in the thorax. The catheter tubing was extended about 40 cm and was attached to a swivel commutator and counterbalanced boom assembly. Following surgery, prophylactic enrofloxacin 5 mg/mL (subcutaneously) and water containing ibuprofen (0.1 mg/mL) were given for 3 days.[5,6,8]

Almorexant Study

Almorexant (ALM) (2*R*)-2-{(1*S*)-6,7-dimethoxy-1-[2-(4-trifluoromethylphenyl)-ethyl]-3,4-dihydro-1Hisoquinolin-2-yl}-*N*-methyl-2-phenyl-acetamide), a dual orexin receptor antagonist (Actelion Pharmaceuticals, Ltd., Allschwil, Switzerland) was dissolved in 0.25% methylcellulose solution in water. Vehicle control was prepared with 0.25% methylcellulose solution in water alone. Almorexant (300 mg/kg) was delivered at 5 mL/kg final volume.[8,16] The effect of ALM on sleep was studied on five AO rats and five control rats. Chronic ALM study: To explore the role of ALM on growth parameters, four groups were used: (1) AO + ALM (n = 5), (2) AO + vehicle (n = 5), (3) control + ALM (n = 5), (4) control + vehicle (n = 5).

Sleep-Wake Activity

Sleep was recorded 49 days following surgery when the animals had acclimatized to the recording environment (n = 12 controls and n = 11 AO). Raw EEG and EMG outputs from the skull and skeletal muscle electrodes were sampled at 250 Hz, filtered at 0.5–40 Hz and 10–250 Hz, respectively, using the DSI system. Vigilance states were scored using DSI NeuroScore (version 2.1 software) and edited visually for 10-sec epochs on the basis of the predominant state within the epoch.[6,8,39] The duration of sleep-wake states was calculated for 12-h light and dark, and for the whole 24 h. The states of vigilance were categorized as: (1) Wake, (2) slow wave sleep (SWS), and (3) paradoxical sleep (PS). SWS – high-amplitude EEG waves, lack of body movement, and predominant EEG power in the delta range (0.5–4.0 Hz) interrupted by low-voltage fast EEG activity (spindles, 6–15 Hz) and continuous (> 70% epoch) high-amplitude slow cortical waves (0.5–4 Hz) with reduced EMG and motor activity. PS: highly regular low-amplitude EEG, dominance of theta activity with corresponding high fast theta (5.0–8.0 Hz) power, general lack of body movements with occasional twitches; Wake: less regular low-amplitude EEG, lack of visible theta dominance, and frequent body movements. The power density values for 0.5–4.0 Hz during were integrated and used to calculate slow wave activity during non-rapid eye movement sleep (n = 10 controls and n = 8 AO).[6,8]

Table 1—Primer sequences used for genes studied.

	Forward Primer	Reverse Primer
IGF-1	CTTGTTTCCTGCACTTCCTCT	CGCTGAAGCCTACAAAGTCA
Sox9	CGTCAACGGCTCCAGCA	TGCGCCCACACCATGA
Type II collagen	CCCAGAACATCACCTACCAC	GGTACTCGATGATGGTCTTG
Type X collagen	CCCAGGGTTACCAGGACCAA	GTTCACCTCTTGGACCTGCC
Aggrecan	GACCAGGAGCAATGTGAGGAG	CTCGCGGTCGGGAAAGT
MMP-13	TGGAGTTATGATGATGCTAACCAGAC	TGTCGCCAATTCCAGGGA
RANKL	GAGCGTSCCTGCGGACTATC	AGGGAAGGGTTGGACACC
Osteocalcin	GAGCTAGCGGACCACATTGG	CCTAAACGGTGGTGCCATAGA
β-Actin	CGTCATCCATGGCGAACT	CCCGCGAGTACAACCTTCT

IGF-1, insulin-like growth factor; MMP-13, matrix metallopeptidase 13; RANKL, receptor activator of nuclear factor kappa-B ligand; Sox9, Sry-related transcription factor nine.

Food Intake

Twenty-four-hour food intake expressed as grams of food/kg of body weight was measured 2 days before animal sacrifice (n = 11 in each group).[8,35] Animals were given 40 g/day (> 40% of maximal daily food intake) of standard rodent chow (Harlan, Jerusalem, Israel). Calories were provided by protein (29.9%), fat (13.4%), and carbohydrate (56.7%) with 13% moisture; energy 3.95 (kcal/kg). Food was placed into the feeder at the beginning and any remaining at the end of each 24-h period was weighed. Any visible food in the cage was scavenged and included in the measurements.[8,35]

Arterial Blood Gas

In undisturbed animals a single sample for blood gas was drawn 2 h after lights on 45 days post-surgery (n = 6 in each group). Blood gas samples of 100 μL were drawn in a preheparinized syringe, placed on ice, and immediately analyzed on a blood gas analyzer (RAPID Point 500, Siemens, Erlangen, Germany).

Magnetic Resonance Imaging

We used a high performance 1T compact M2 MRI, 35 mm ID solenoid coil (Aspect Imaging, Shoham, Israel).[8] Images were acquired with a gradient spin echo sequence, with repetition time (TR)/echo time (TE)/NEX = 13.4/3/2. Multislice axial scans were collected with a 5-cm field-of-view and data matrix of 256 × 256, resulting in 50/256 = 0.195 mm in-plane resolution, slice thickness of 1 mm. Region growing algorithm was used for segmentation of two objects: trachea and the circumferential silicon band used for the trachea-narrowing (n = 7 in each group).

Histology

The left tibia was fixed in 4% formalin for 48 h and decalcified in a solution containing EDTA (Gadot Laboratory Supplies, Netanya, Israel) for 7–9 days at room temperature. Five-μm-thick longitudinal sections were cut and collected on Superfrost™ Plus slides for histology staining of Masson trichrome,[40] safranin O,[41] and hematoxylin and eosin.[5] Total growth-plate width and proliferative and hypertrophic zones' width were measured as previously described (n = 8 in each group).[30] Two sections per animal at 15 different fields per section were analyzed.

Immunohistochemistry

Immunohistochemistry staining was performed using a protocol described previously by our laboratory (n = 6 in each group).[30] Anti-goat OX1R and anti-rat Sox9 (Santa Cruz Biotechnology, Santa Cruz, CA, USA) were used for the immunohistochemistry staining. For image processing, Cellsens Entry software (MATIMOP, Tel Aviv, Israel) was used. All the experiments and observations were repeated at least three times.

Quantitative Real-Time Polymerase Chain Reaction

Assays were performed with power SYBR green polymerase chain reaction (PCR) master mix (Applied Biosystems) as previously described[42] using the ABI Prism 7300 Sequence Detection System (Applied Biosystems). Primers for quantification of collagen type II, collagen type X, aggrecan, MMP13, IGF1, RANKL, osteocalcin, β-actin and IGF-I (n = 7 in each group) (Sigma-Aldrich, Rehovot, Israel) are summarized in Table 1. Each sample was analyzed in triplicate in individual assays. The specificity of the reaction is given by the detection of the melting temperatures (Tms) of the amplification products immediately after the last reaction cycle. The target gene expression value was calculated by the DDct method after normalization with a housekeeping gene (beta-actin).

Table 2—Arterial blood gases and serum biochemistry.

	Control	Obstructive
PO_2 (mmHg)	88.6 ± 2.8	87.2 ± 3.2
PCO_2 (mmHg)	38.8 ± 3.3	42.8 ± 3.1
pH (units)	7.5 ± 0.01	7.45 ± 0.01
HCO_3^- (mEq/L)	23.5 ± 1.1	25.5 ± 1.7
Calcium (mg/dL)	10.6 ± 0.3	10.9 ± 0.7
Phosphate (mg/dL)	8.0 ± 0.6	8.9 ± 1.2
Iron (μg/dL)	187.6 ± 19.2	169.3 ± 67.8
Glucose (mg/dL)	199.5 ± 64.5	220.6 ± 92.8
Triglycerides (mg/dL)	52.1 ± 22.1	62.2 ± 21.7
Protein total (g/dL)	5.7 ± 0.3	5.2 ± 0.6
Urea (mg/dL)	45.6 ± 5.28	45.9 ± 8.6
Creatinine (mg/dL)	0.35 ± 0.04	0.31 ± 0.01
IGF-1 (ng/mL)	2128.3 ± 48	1316.0 ± 154.2*
Corticosterone (ng/mL)	96.3 ± 7.4	100 ± 0.5
Ghrelin (ng/mL)	0.4 ± 0.1	1.1 ± 0.27*
Leptin (ng/mL)	0.85 ± 0.06	0.48 ± 0.13*

Arterial blood gases, serum biochemistry corticosterone, ghrelin, and leptin (n = 6 in each group); IGF-1 (n = 7 in each group). *P < 0.001; unpaired two-tailed *t*-test. Values are mean ± standard deviation. HCO_3, calculated arterial bicarbonate; IGF-1, insulin-like growth factor 1; PCO_2, arterial CO_2 pressure; pH, arterial pH; PO_2, arterial O_2 pressure.

Western Immunoblot Analysis

The following antibodies were used for evaluation of the GP extracts: OX1R (n = 11 controls and n = 10 AO), ghrelin (n = 9 controls and n = 7 AO), Sox9 (n = 9 controls and n = 7 AO), growth hormone (GH) secretagogue receptor (GHSR) 1a (n = 9 controls and n = 7 AO), PPARγ (n = 7 controls and n = 9 AO), and p-AKT (n = 7 in each group) (Santa Cruz Biotechnology), AKT (Cell Signaling Technology, Danvers, MA, USA), and β-actin (MP Biomedical Solon, OH, USA). The full protocol is described in our previous publication.[42]

Serum Biochemistry and Endocrine

Serum biochemistry was analyzed by the Biochemistry Laboratory of Soroka Medical Center (Beer-Sheva, Israel) (n = 8 in each group). Serum IGF-1, corticosterone, and ghrelin (n = 6 in each group) were determined by specific enzyme-linked immunosorbent assay kits according to the manufacturer's instructions. The low and high detection limits for IGF-I were 25-3000 ng/mL intracoefficient and intercoefficient of variation (CV) was 4.8% (Diagnostic System Laboratories Inc. Webster, TX, USA). The low and high detection limits for leptin were 62.5 and 4,000 pg/mL (R&D Systems, Minneapolis, MN, USA), and the intra-assay and interassay CVs were < 4 and 6%, respectively.

The low and high detection limits for ghrelin were 0.04 and 10 ng/mL (Merck Millipore, Rosh Haayin, Israel), and the intra-assay and interassay CVs were 1.1% and 3.2%, respectively. The low and high detection limits for corticosterone were 0.3 and 100 ng/ml (Assaypro, Charles, MO, USA) and the intra-assay and interassay CVs were < 5 and 6%, respectively. Values that fell below or above the range of assay detection were set equal to the lower or upper limit of sensitivity, respectively.

Micro CT Scanning and Analysis

Femurs were scanned using a μ-CT machine (Skyscan 1174 v2. Bukner, Kontich, Belgium) at 27 μm resolution, using a 0.25 mm aluminum filter. X-ray tube peak potential was 50 kV and X-ray intensity 800 μA. Analysis of trabecular bone was performed along 2 mm, starting 0.4 mm below the distal growth plate's border (n = 9 controls and n = 8 AO). Each image was reconstructed from 498 slices 0.2 μm in width.[43] Structural indices were calculated using the Skyscan CT Analyzer (CTAn) software. A set of 2 hydroxyapatite (HA) phantoms were scanned and used for calibration of bone mineral density (BMD). Trabecular bone volume per total volume (BV/TV), mean trabecular thickness (Tb.Th), mean trabecular number (Tb.N), and mean trabecular separation (Tb.Sp) indices were computed using a marching-cubes algorithm. For cortical bone, 2 mm in the direction of the metaphysis were taken as an offset from the GP and a 1 mm area was chosen for cortical bone analysis. Cortical BV/TV and BMD were calculated.

Experimental Schedule

Tracheal narrowing or sham control surgery was performed on 22-day-old rats (day 0) and animals were followed for 5 to 7 w; a period comparable to > 15 y in humans.[39] Trachea MRI scanning was performed 2 w postsurgery. Sleep (recorded for 24 h), food intake, and arterial blood gases were measured 4 days before animal sacrifice. The effect of ALM on sleep was studied on a separate group. Baseline vehicle study was performed on day 46 and ALM (300 mg/kg) study was performed on day 47; vehicle or ALM were administered as oral gavage at lights on.[8,16] For the chronic ALM study separate groups of animals were used. Animals were administered ALM or vehicle at lights on for 8 consecutive days starting on day 1 as oral gavage at lights on. Data were collected on day 8, 2 h after the last administration of ALM or vehicle. Animals fasted overnight before sacrifice. At sacrifice animals were anesthetized, the serum was collected, and tibia and femur were removed and stored at –80°C. The small intestine length was measured between the pylorus and the junction with the cecum immediately after sacrifice.[8] Micro CT scanning was performed postmortem.

Data Analysis

Significance was analyzed by unpaired Student *t*-test; paired Student *t*-test was used to analyze the effect of ALM or vehicle on sleep during the first 8 h of lights-on. Two-way analysis of variance for repeated measures was used to determine significance between time and group using *post hoc* comparisons by Student-Newman-Keuls test. Null hypotheses were rejected at the 5% level.

RESULTS

Following AO surgery trachea diameter was narrowed by about 60% compared to the control group (P < 0.001; Figure 1A and 1B). Mean arterial blood gas tensions in undisturbed AO animals were statistically similar to those of the control group and no signs of hypoxia in AO animals were observed (Table 2).

Mean serum leptin levels deceased by 44% ($P < 0.001$; Table 2) and mean serum ghrelin levels increased by 275% ($P < 0.001$; Table 2) in the AO group compared to the control group. Mean daily food intake increased by 23% ($P < 0.05$) from 83.4 ± 12.6 g/kg/day to 102.6 ± 0.04 g/kg/day in the control and obstructive groups, respectively. Small intestine length to body length ratio was 17% longer in the AO group ($P = 0.001$; Table 3), consistent with increased intestine surface area to increase absorption of water and nutrients. Significant changes were measured in sleep-awake pattern: The time course of normalized slow wave activity power in the control group showed high power at the beginning of the light period, followed by a decline toward dark onset, and a gradual increase in power during the 12-h dark period (Figure 1C). In contrast, the daily course of slow wave activity power was flat in the AO group and there were no significant changes across the day ($P < 0.01$; Figure 1C). The AO group was awake 32% longer ($P < 0.001$) during 12-h lights on, time spent in SWS was lower by 14% ($P = 0.005$), and there was 57% less PS ($P < 0.001$) (Figure 1D). During 12 h of lights off (active period) the AO group was awake 11% less time ($P = 0.02$), spent 56% more time in SWS ($P < 0.005$), and 25% less time in PS ($P < 0.002$) (Figure 1D).

Growth Plate OX1R and Ghrelin Expression

OX1R protein in the GP was higher in the AO group as determined by immunohistochemistry (Figure 2A) and Western blot analysis (Figure 2B). OX2R protein and messenger RNA (mRNA) were undetected in the growth plate. Ghrelin protein in the GP was reduced by 34% ($P < 0.001$; Figure 2C); growth hormone secretagogue receptor 1a (GHSR1a) mRNA and GHSR1a protein were reduced by 92% ($P < 0.001$; data not shown) and 31% ($P < 0.01$; Figure 2D), respectively. In contrast,

Table 3—Growth and microcomputed tomography analysis.

	Control	Obstructive	P
Body weight (g)	299.7 ± 29	162.9 ± 53.2	0.001
Body length (cm)	20 ± 1.2	16.1 ± 1.8	0.001
Intestine length (cm)	121.1 ± 4.6	115 ± 7.6	0.030
Intestine length/body length	6.01 ± 0.4	7.2 ± 0.5	0.002
Tb.BV (mm^3)	2.62 ± 0.24	1.56 ± 0.28	0.010
Trabecular BV/TV (%)	15.6 ± 1.05	10.3 ± 1.88	0.029
Tb.N (1/mm)	1.4 ± 0.08	1.0 ± 0.13	0.023
Tb.Sp (mm)	0.67 ± 0.04	0.95 ± 0.1	0.033
Cortical BV (mm^3)	1.62 ± 0.03	1.2 ± 0.06	0.001
Cortical BV/TV (%)	34.8 ± 0.7	31.8 ± 0.9	0.024
Cortical BMD (g/cm^3)	0.8 ± 0.006	0.82 ± 0.009	n.s.

Body weight, body length, food intake, and intestine length (n = 11 in each group); micro-computed tomography analysis (n = 9 controls and n = 8 airway obstructed). P value was determined by unpaired two-tailed *t*-test. BMD, cortical bone mineral density; BV, bone volume; cortical BV/TV, bone volume/tissue volume; IL/BL, intestine length/body length; n.s., not significant; Tb.Bv, trabecular number/bone volume; Tb.N, trabecular number; Tb.Sp, trabecular separation; trabecular BV/TV, bone volume/tissue volume; TV, tissue volume.

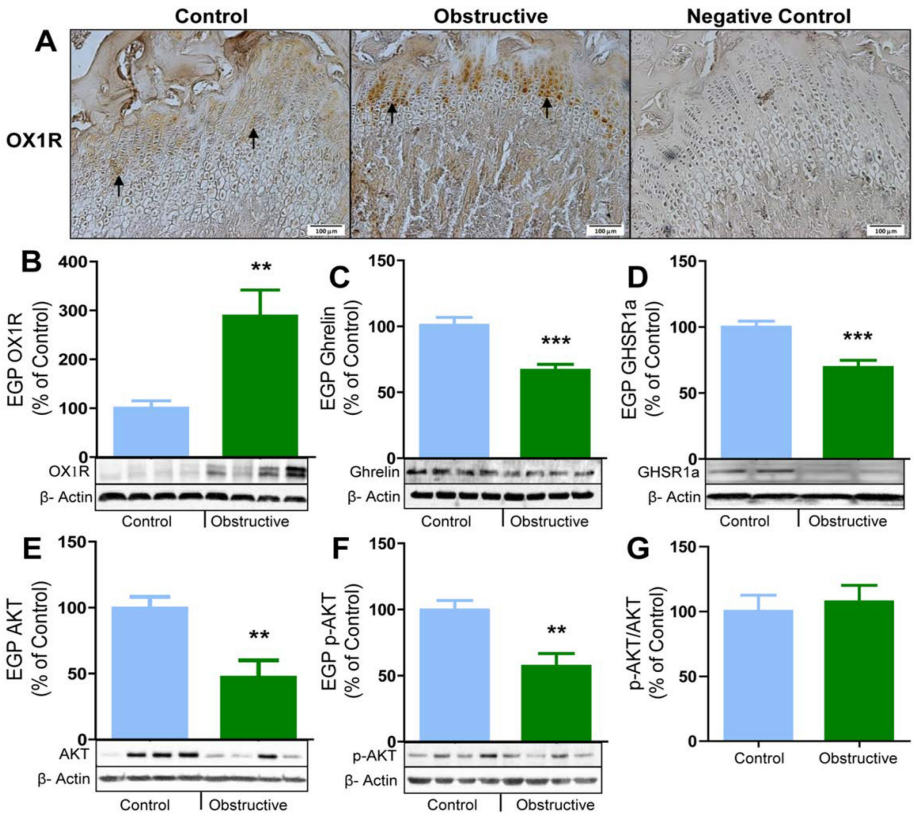

Figure 2—Growth plate OX1R, GHSR1a, and AKT expression. **(A)** Orexin receptor 1 (OX1R) protein distribution in the growth plate tested by immunohistochemistry, Bar = 100 μM (n = 7 in each group). Arrows point to OX1R positive stained chondrocytes; **(B)** Growth plate (EGP) OX1R protein determination by Western blot analysis (n = 11 controls and n = 10 airway obstructed [AO]); **(C)** Growth plate ghrelin protein determination by Western blot analysis (n = 9 controls and n = 7 AO); **(D)** Growth plate growth hormone secretagogue receptor 1a (GHSR1a) protein determination by Western blot analysis (n = 9 controls and n = 7 AO); **(E)** Growth plate AKT protein determination by Western blot analysis (n = 7 in each group); **(F)** Growth plate phosphorylation of AKT (p-AKT) determination by Western blot analysis (n = 7 in each group); **(G)** p-AKT/AKT ratio (n = 7 in each). **P < 0.01, ***P < 0.001 unpaired two-tailed *t*-test.

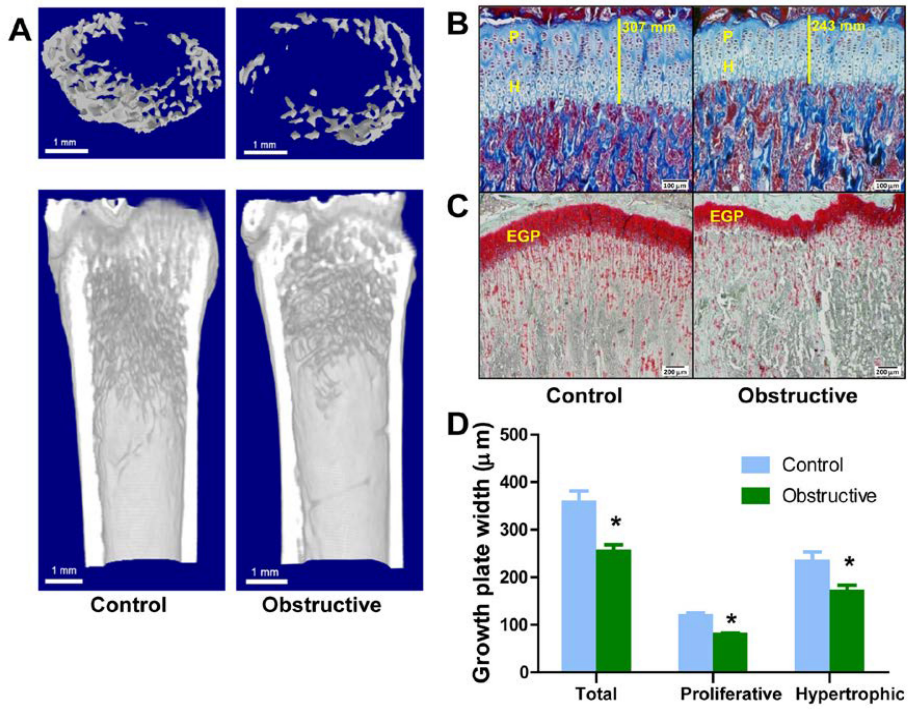

Figure 3—Somatic growth and bone architecture. **(A)** Representative images of the trabecular bone of the femur metaphysis and the entire proximal femur. **(B)** Masson's trichrome staining of growth plate and primary ossification center, which stains nuclei black, collagen blue. H, hypertrophic; P, proliferative. Horizontal bar = 100 μM. Vertical yellow bar indicate growth plate width. **(C)** Safranin O stain, orange-red colors, cartilage proteoglycans, Bar = 200 μM. **(D)** Growth plate width (μM) (n = 8 in each group). *P < 0.05 unpaired two-tailed *t*-test.

the level of serum ghrelin, which largely derives from the stomach, increased in the AO group (Table 2). Growth plate AKT protein and phosphorylation of AKT (P-AKT) were significantly reduced by 53% and 43%, respectively, in the AO group ($P < 0.01$; Figures 2E and 2F); no change in P-AKT/AKT was observed (Figure 2G).

Body Growth

Body weight and body length of the AO group were 46% and 20% less than in control group, respectively ($P < 0.001$; Table 3). A three-dimensional reconstructed micro-CT image of distal trabecular femur showed that the AO group has low bone mass (Figure 3A). Quantification of bone structure and architecture (Table 3) demonstrated that the trabecular bone volume to total volume (BV/TV) ratio decreased by 34% ($P = 0.029$) in the AO group. A similar pattern was seen in trabeculae number (Tb.N); in addition, trabecular separation (Tb.Sp) increased by 42% ($P = 0.033$) in the AO group. Cortical BV/TV ratio decreased by 9% ($P = 0.024$) in the AO group. However, cortical BMD was unchanged. Growth plate width decreased by 27% ($P < 0.001$) in the AO group (Figures 3B and 3D) and all AO group histology slides showed a similar difference (Figure 3B). Total growth plate, and proliferative and hypertrophic zones' width significantly decreased by 29% ($P < 0.001$), 33% ($P < 0.001$), and 27% ($P < 0.001$), respectively, in the AO group (Figure 3D). Safranin O, which is used for staining cartilage proteoglycan, indicating the ability of the GP to produce extracellular matrix, showed decreased staining intensity of the primary spongiosa in the AO group (Figure 3C) and similar findings were found in all AO animals.

Growth Plate Mediator Factors

The transcription factor Sox9 as observed by both mRNA and protein measurements was significantly reduced in the AO group (Figures 4A–4C). Collagen type II and aggrecan mRNAs production were also reduced by 60% (Figures 5A and 5B), and type X collagen mRNA that is produced by hypertrophic chondrocytes was decreased by 50% ($P < 0.001$; Figure 5C). Growth plate MMP-13 mRNA increased by 80% ($P < 0.01$; Figure 5D) and RANKL mRNA decreased by 50% (Figure 5E). Osteocalcin mRNA decreased by 73% in the AO group ($P < 0.001$; Figure 5F). Serum IGF-1 level decreased by 38% ($P < 0.001$; Table 2) and GP IGF-1 mRNA decreased from 1.14 ± 0.16 (fold of control) to 0.72 ± 0.09 (fold of control) in the AO group ($P = 0.03$). The 250% elevation of OX1R was associated with bone mass loss (Figure 3A and Table 3), 520% increase of PPARγ protein (Figure 4D), and increased marrow adipose (Figure 4E). All AO group rats showed obvious difference of marrow adipose compared to the control group by visual examination of the histology slides.

Effect of Almorexant on Sleep and Growth Plate Histomorphology

The effect of dual orexin antagonist on sleep was explored (Figure 6A). Acute administration of ALM significantly decreased wake duration and increased SWS duration in both groups ($P < 0.05$) but this effect was more robust in the AO group. Wake duration in the ALM-treated AO group decreased to levels similar to those of baseline vehicle control values. Almorexant administration for 8 days did not the affect body weight of AO group relative to the vehicle AO group (81 ± 5.2 g, 83 ± 9.1 g, 58.8 ± 3.8 g, and 60.2 ± 5.5 g in control + vehicle, control + ALM, AO + vehicle, and AO + ALM, respectively). Almorexant significantly improved growth plate of AO group width by 28% in comparison to the vehicle AO group ($P = 0.05$; Figures 6B and 6C). Almorexant improved the proliferative zone of the AO group by 21% relative to the vehicle AO group ($P = 0.013$) (131.3 ± 8.7 μM, 125.2 ± 10.3 μM, 72.0 ± 8.2 μM, and 87.7 ± 5.1 μM in control + vehicle, control + ALM, AO + vehicle, and AO + ALM, respectively). Almorexant did not affect the hypertrophic zone of AO group rats (327.9 ± 67.6 μM, 347.4 ± 30.5 μM, 174.1 ± 44.3 μM, and 212.4 ± 30.0 μM

in control + vehicle, control + ALM, AO + vehicle, and AO + ALM, respectively). Almorexant increased GP Sox9 mRNA in comparison to the vehicle AO group ($P < 0.005$) to levels similar to the vehicle control group (Figure 6D).

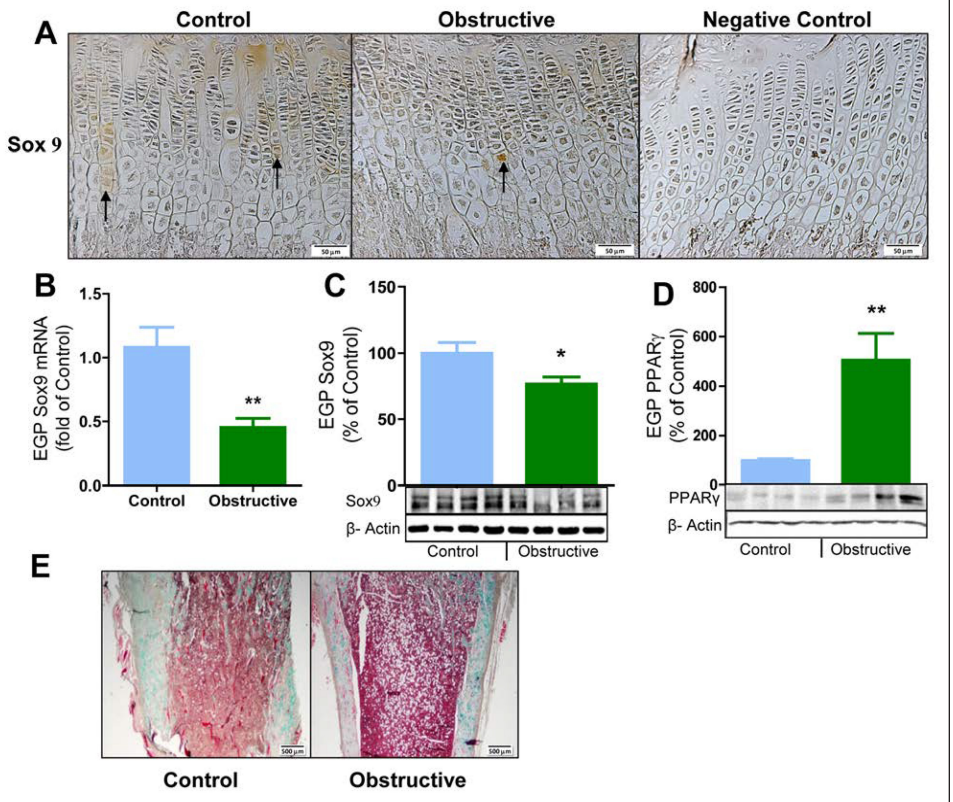

Figure 4—Growth plate early bone development markers. **(A)** Sox9 protein distribution in the growth plate tested by immunohistochemistry. Bar = 50 μM. Arrows point to Sox9 positive stained chondrocytes. **(B)** Growth plate (EGP) Sox9 messenger RNA level. **(C)** Growth plate Sox9 protein determination by Western blot analysis (n = 9 controls and n = 7 airway obstructed [AO]). **(D)** Growth plate peroxisome proliferator-activated receptor gamma (PPARγ) protein determination by Western blot analysis (n = 7 controls and n = 9 AO). **(E)** Marrow fat cells, Movat modified pentachrome staining. Bar = 500 μM (n = 8 in each group). **P < 0.01, ***P < 0.001 unpaired two-tailed *t*-test.

DISCUSSION

SDB is a common condition and, if left untreated, may lead to a cascade of complex endocrine derangements that can affect sleep, longitudinal growth, energy metabolism,[1,44–46] and bone mass in adults,[7] by mechanisms that are poorly understood. To our knowledge, this study is the first to show that enhanced expression of orexin and OX1R plays a role in respiratory-induced sleep (Figures 1C and 1D) and growth abnormalities (Figure 3), probably by altering local ghrelin (Figures 2C–2G). Administration of ALM normalized sleep and considerably improved GP width in AO animals (Figure 6).

This study explored the effects of AO on sleep and GP metabolism/architecture from weaning to adulthood. The AO group demonstrated audible wheezing, mainly after activity, but no signs of gasping or stress were observed during routine activity.[8] Serum corticosterone level, a marker for stress, was similar in both groups (Table 2). Arterial blood gases measured in unrestrained animals were in the normal physiological range, indicating animals are maintaining their normal ventilation and pO_2 (Table 2).[34,35] Both inspiratory and expiratory loading were induced (Figure 1A), which may resemble subglottic stenosis in children and not be exclusively sleep related, whereas in human SDB, upper airway loading is mainly inspiratory and sleep related.[1,46] This model also has implications for this condition because, like in SDB, AO animals exhibited substantial temporal alterations in sleep-wake activity, indicating fragmented sleep,[39] and as in children with sleep apnea, growth retardation.[5] AO surgery (Figures 1A and 1B) led to 40–100% elevation of tracheal resistance,[5,6,35] which was associated with adaptive changes in the respiratory system, such as large swings in pleural pressure and increased respiratory muscle contractility.[32–35] These adaptations are essential for proper ventilation maintenance, especially during sleep, a condition where respiratory muscle force may not be sufficient to support ventilation. Orexin has a key role as orchestrator of brain states and adaptive behaviors; both arousal and breathing centers receive stimulatory inputs from orexin neurons.[16] Elevation of hypothalamic orexin in AO animals[8] (see next paragraph) was found to play a role in this respiratory adaptive response. Administration of ALM to AO animals induced breathing difficulties and failure to maintain upper airway patency, while it did not affect sleep or breathing in control animals.[8] The reduction of hypothalamic growth hormone-releasing hormone content underlies both the abnormal SWS and growth impediment in AO animals.[6] Stimulation of hypothalamic growth hormone-releasing hormone with ritanserin (5-HT2 receptor antagonist) restored sleep and the growth hormone axis to control values; however, impediment of bone elongation only partially improved,[5,6] indicating that other pathways are involved this growth retardation.

This study is the first to show that local elevation of OX1R (Figures 2A and 2B) is associated with suppressed GP metabolism (Figures 2 and 4) and growth (Figure 3 and Table 3) during chronic inadequate sleep induced by upper airway loading in rats (Figure 1). Sleep is essential for normal growth and development. The elevation of OX1R and altering of GP orexin and ghrelin during chronic inadequate respiratory-induced sleep disorder was possibly an adaptive response essential to preserve vital organ function (Table 2) at the "cost" of growth retardation. Sleep loss in AO animals is associated with 65% elevation of hypothalamic orexin content.[8] Almorexant administration restored sleep and increased GP width (Figure 6). This

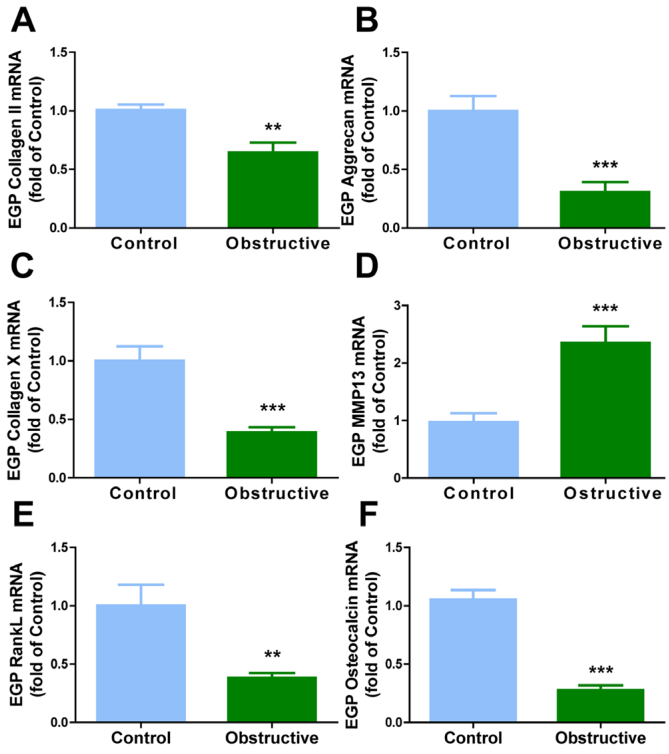

Figure 5—Growth plate bone formation messenger RNA (mRNA) markers. Epiphyseal growth plate (EGP) mRNAs: **(A)** Collagen II. **(B)** Aggrecan. **(C)** Collagen X. **(D)** Matrix metalloproteinase 13 (MMP-13). **(E)** Receptor activator of nuclear factor kappa-B ligand (RANKL). **(F)** Osteocalcin. Values were determined by quantitative real time polymerase chain reaction. For A–F (n = 7 in each group). *P < 0.05, **P < 0.01, ***P < 0.001 unpaired two-tailed *t*-test.

increased GP width was not related to changes in body weight because body weight was not affected by ALM relative to vehicle AO animals. It is unclear what causes the considerable elevation of OX1R in AO animals. Further studies are needed to explore the mechanism leading to upregulation of OX1R in the GP in AO animals. Because bone elongation requires longer than 1 w to complete, further studies are needed to explore the effect of long-term administration of OX1R antagonist on bone growth/metabolism. Elevation of serum leptin level plays a critical mediator role in central bone mass regulation by suppressing bone formation.[47,48] In the current study, serum leptin levels were dramatically reduced in AO animals (Table 2) due to reduction of body adipose tissue.[8] Thus, if serum leptin was the only factor, its reduction should lead to increased bone mass. Our observation of bone mass reduction in AO despite low circulatory leptin level, suggest that the peripheral OX1R activation in the GP has a more dominant influence on growth in AO rats than activation of brain OX2R. The increased food intake in our study was a physiological adaptation to provide energy needed to sustain the additional wakefulness[49,50] and the increased work of breathing.[2,32] The increase in energy demands was related to increased hunger-stimulating hormone ghrelin and decreases in the satiety hormone leptin, leading to increased food intake[51,52] (Table 3). If increased energy demands will not be met with increased caloric intake, weight loss would ensue in adult animals[47,49] and growing animals will gain less body weight, as occurred in the current study. Further studies are needed to explore the whole-body energy expenditure using an open-circuit indirect calorimeter.[47] SDB in humans is associated with insufficient sleep and increased energy consumption. In addition to loss of SWS and rapid eye movement sleep,[39,45,51,53] this disorder involves frequent arousals and increased nighttime energy expenditure,[2,44] which may lead to compensatory changes in daytime energy intake and physical activity.[1,44,52,54] SDB and low bone mass are two prevalent conditions in aging adults.[7] It was previously found that SDB via decreased sleep quality, nocturnal hypoxia, inflammation, etc. can affect bone metabolism and bone mass.[7] However, this study did not discuss the possible role of orexin on bone metabolism/architecture.[15]

As in mice,[15] expression of only OX1R and not of OX2R was found in rat tibia. Earlier studies showed that OX1R could regulate ghrelin content locally in the bone.[15] It was established that several signaling pathways of ghrelin, including the AKT-dependent pathway, play important roles in chondrogenesis and osteoblastogenesis.[15,17,18,55–57] Ghrelin is expressed in both proliferative and mature chondrocytes[58] and acts as a local growth factor.[59] In our study the reduction of GP ghrelin protein (Figure 2A) and its receptor (Figure 2D) was associated with decreased GP width and trabecular bone mass reduction (Figure 3 and Table 3). Moreover, OX1R is suppressed during osteoblast differentiation and elevated during adipocyte differentiation.[15] We found that elevated OX1R (Figures 2A and 2B) is associated with increased bone PPARγ protein and marrow adipose (Figures 4D and 4E) and decreased Sox9 mRNA and protein (Figures 4A–4C). Sox9 plays important roles in chondrogenesis differentiation.[28] PPARγ is a transcription factor essential for adipocyte differentiation processes in adipose tissue, liver, and bone marrow.[28,60] Orexins activate marrow PPARγ that causes bone mass loss and increased adipogenesis.[20–23,60] Sox9 downregulation will promote adipocyte differentiation in mesenchymal cells, a process that is activated by PPARγ.[61] Mice heterozygous for PPARγ deficiency had low marrow fat and high bone mass[23]; pharmacological inhibition of PPARγ increases osteoblastogenesis and enhances bone mass in mice.[62]

Using micro-CT scanning we investigated trabecular and cortical bone architecture (Figure 3A and Table 3). Trabecular bone is the main product of endochondral ossification, which leads to long bone elongation, whereas cortical bone is the product of intramembranous ossification, which leads to bone width expansion.[63] Growth gain inversely correlates with increased tracheal resistance in AO animals.[5] In the current study, growth retardation in the AO group was associated with narrowing of both proliferative and hypertrophic zones and loss of trabecular bone mass. This growth abnormality could be related to reduced function of the GP and the endochondral ossification process. The expression of endochondral ossification markers[64] such as Sox9, collagen type II and X, RANKL, and osteocalcin nRNAs were all decreased in AO animals (Figure 5). Administration of orexin antagonist (ALM 300 mg/

kg) for 8 days increased GP Sox9 mRNA and protein level in both groups (Figure 6). Further studies are needed to explore the role of orexin on Sox9. In our study Sox9 mRNA and protein was decreased (Figures 4A and 4B), as were the levels of AKT. The PI3K/AKT axis controls aggrecan gene expression, in part by modulating Sox9 expression and activity in rat nucleus pulposus cells.[65] Postnatal inactivation of Sox9 growth retardation is characterized by decreased proliferation of GP chondrocytes and reduced aggrecan and collagen type II expression.[66] A similar phenotype is seen in our AO animals. Interestingly, Sox9 has been shown to promote chondrocyte survival by directly binding and activating PI3K promoter and thus activating AKT.[67]

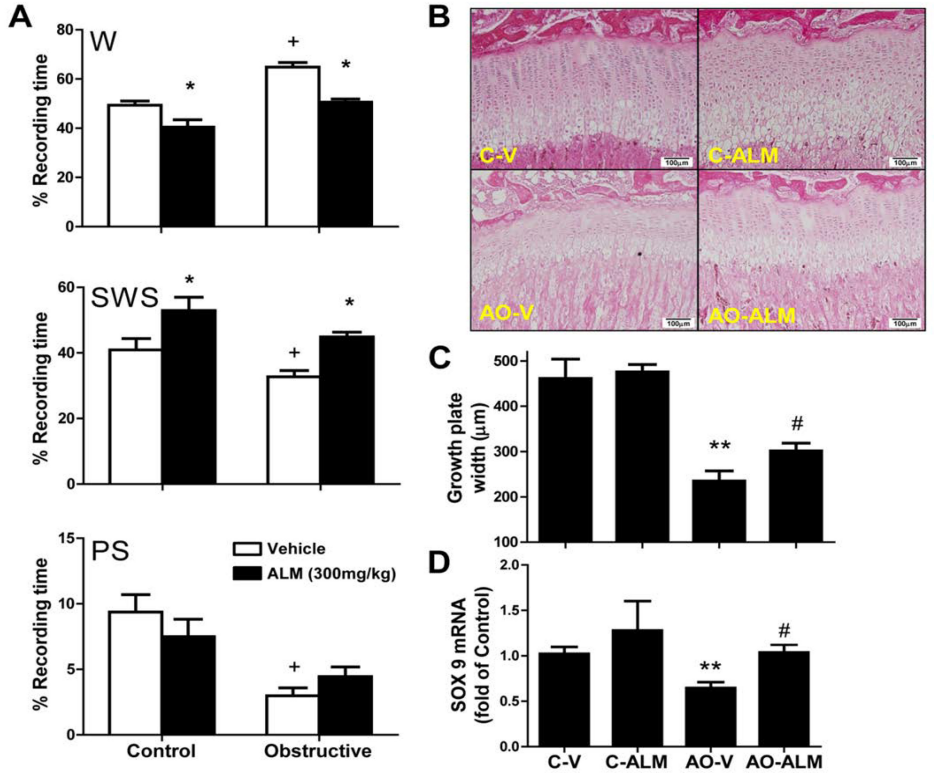

Figure 6—Effect of dual orexin receptor antagonist on sleep and growth plate morphology. **(A)** Effect of almorexant (ALM, 300 mg/kg) on spontaneous sleep (n = 5 in each group); Bars represent mean duration of wake (W), slow wave sleep (SWS), and paradoxical sleep during 12-h lights-on period. On day 1, animals were given vehicle (white bars) (0.25% methylcellulose solution in water) and on day 2 (black bars), animals were administered ALM at lights on. **(B)** Growth plate stained with hematoxylin and eosin; **(C)** growth plate width (mM) and Sox9 mRNA level **(D)** (n = 5 in each group). *P < 0.05 comparing day one with day two paired two-tailed t-test. +P < 0.05 comparing vehicle obstructive (AO-V) with vehicle control (C-V) group, unpaired two-tailed *t*-test. #P < 0.05 comparing AO-ALM with AO-V, unpaired two-tailed *t*-test. **P < 0.05 comparing AO-V with C-V unpaired two-tailed *t*-test.

Summary

This study shows for the first time that abnormal sleep and growth retardation in AO animals is associated with increased expression of orexin and OX1R, and suppression of GHSR1a and ghrelin in the growth plate. The abnormal sleep in AO animals was associated with slower weight gain, despite elevated food intake, and increased plasma ghrelin and decreased leptin level. The robust increase of PPARγ and reduction in Sox9 was associated with bone architecture abnormalities and growth retardation. These findings indicate that orexin may have potential clinical relevance in growth and sleep impairment in pediatric SDB. Future studies are needed to support this observation.

REFERENCES

1. Marcus CL, Brooks LJ, Draper KA, et al.; American Academy of Pediatrics. Diagnosis and management of childhood obstructive sleep apnea syndrome. Pediatrics 2012;130:e714–55.
2. Marcus CL, Carroll JL, Koerner CB, Hamer A, Lutz J, Loughlin GM. Determinants of growth in children with obstructive sleep apnea syndrome. J Pediatr 1994;125:556–62.
3. Bar A, Tarasiuk A, Segev Y, Phillip M, Tal A. The effect of adenotonsillectomy on serum insulin-like growth factor-I and growth in children with obstructive sleep apnea syndrome. J Pediatr 1999;135:76–80.
4. Tarasiuk A, Segev Y. Chronic upper airway resistive loading induces growth retardation via the GH/IGF-1 axis in pre-pubescent rats. J Appl Physiol 2007;102:913–8.
5. Segev Y, Berdugo-Boura N, Porati O, Tarasiuk A. Upper airway loading induces growth retardation and change in local chondrocyte IGF-I expression is reversed by stimulation of GH release in juvenile rats. J Appl Physiol 2008;105:1602–9.
6. Tarasiuk A, Berdugo-Boura N, Troib A, Segev Y. Role of GHRH in ssleep and growth impairments induced by upper airway obstruction in rats. Eur Respir J 2011;38:870–7.
7. Swanson CM, Shea SA, Stone KL, et al. Obstructive sleep apnea and metabolic bone disease: insights into the relationship between bone and sleep. J Bone Miner Res 2015;30:199–211.
8. Tarasiuk A, Levi A, Berdugo-Boura N, Yahalom A, Segev Y. Role of orexin in respiratory and sleep homeostasis during upper airway obstruction in rats. Sleep 2014;37:987–98.
9. Bonuck KA, Freeman K, Henderson J. Growth and growth biomarker changes after adenotonsillectomy: systematic review and meta-analysis. J Arch Dis Child 2009;94:83–91.
10. Yakar S, Rosen CL, Beamer WG, et al. Circulating levels of IGF-1 directly regulates bone growth and density. J Clin Invest 2002;110:771–81.
11. Chemelli RM, Willie JT, Sinton CM, et al. Narcolepsy in orexin knockout mice: molecular genetics of sleep regulation. Cell 1999;98:437–51.
12. Lin L, Faraco J, Li R, et al. The sleep disorder canine narcolepsy is caused by a mutation in the hypocretin (orexin) receptor 2 gene. Cell 1999;98:365–76.
13. Sakurai T, Amemiya A, Ishii M, et al. Orexins and orexin receptors: a family of hypothalamic neuropeptides and G protein-coupled receptors that regulate feeding behavior. Cell 1998;92:573–85.

14. de Lecea L, Kilduff TS, Peyron C, et al. The hypocretins: hypothalamus-specific peptides with neuroexcitatory activity. Proc Natl Acad Sci U S A 1998;95:322–7.
15. Wei W, Motoike T, Krzeszinski JY, et al. Orexin regulates bone remodeling via a dominant positive central action and a subordinate negative peripheral action. Cell Metab 2014;19:927–40.
16. Li A, Nattie E. Antagonism of rat orexin receptors by almorexant attenuates central chemoreception in wakefulness in the active period of the diurnal cycle. J Physiol 2010;588:2935–44.
17. Zhang R, Murakami S, Coustry F, Wang Y, de Crombrugghe B. Constitutive activation of MKK6 in chondrocytes of transgenic mice inhibits proliferation and delays endochondral bone formation. Proc Natl Acad Sci U S A 2006;103:365–70.
18. Monemdjou R, Vasheghani F, Fahmi H, et al. Association of cartilage-specific deletion of peroxisome proliferator-activated receptor γ with abnormal endochondral ossification and impaired cartilage growth and development in a murine model. Arthritis Rheum 2012;64:1551–61.
19. Skrzypski M, T Le T, Kaczmarek P, et al. Orexin A stimulates glucose uptake, lipid accumulation and adiponectin secretion from 3T3-L1 adipocytes and isolated primary rat adipocytes. Diabetologia 2011;54:1841–52.
20. Wei W, Wan Y. Thiazolidinediones on PPARγ: the roles in bone remodeling. PPAR Res 2011;2011:867180.
21. Ahmadian M, Suh JM, Hah N, et al. PPARγ signaling and metabolism: the good, the bad and the future. Nat Med 2013;19:557–66.
22. Sugii S, Olson P, Sears DD, et al. PPARgamma activation in adipocytes is sufficient for systemic insulin sensitization. Proc Natl Acad Sci U S A 2009;106:22504–9.
23. Akune T, Ohba S, Kamejura S, et al. PPARgamma enhances osteogenesis through osteoblast formation from bone marrow progenitors. J Clin Invest 2004;113:846–55.
24. Fahmi H, Martel-Pelletier J, Pelletier JP, Kapoor M. Peroxisome proliferator-activated receptor gamma in osteoarthritis. Mod Rheumatol 2011;21:1–9.
25. Woods A, Wang G, Beier F. Regulation of chondrocyte differentiation by the actin cytoskeleton and adhesive interactions. J Cell Physiol 2007;213:1–8.
26. Olsen BR, Reginato AM, Wang W. Bone development. Annu Rev Cell Dev Biol 2000;16:191–220.
27. Erlebacher A, Filvaroff EH, Gitelman SE, Derynck R. Toward a molecular understanding of skeletal development. Cell 1995;80:371–8.
28. Mackie EJ, Ahmed YA, Tatarczuch L, Chen KS, Mirams M. Endochondral ossification: how cartilage is converted into bone in the developing skeleton. Int J Biochem Cell Biol 2008;40:46–62.
29. Shiomi T, Lemaître V, D'Armiento J, Okada Y. Matrix metalloproteinases, a disintegrin and metalloproteinases, and a disintegrin and metalloproteinases with thrombospondin motifs in non-neoplastic diseases. Pathol Int 2010;60:477–96.
30. Troib A, Landau D, Kachko L, Rabkin R, Segev Y. Epiphyseal growth plate growth hormone receptor signaling is decreased in chronic kidney disease-related growth retardation. Kidney Int 2013;84:940–9.
31. Hino K, Saito A, Kido M, et al. Master regulator for chondrogenesis, Sox9, regulates transcriptional activation of the endoplasmic reticulum stress transducer BBF2H7/CREB3L2 in chondrocytes. J Biol Chem 2014;289:13810–20.
32. Tarasiuk A, Scharf SM, Miller MJ. Effect of chronic resistive loading on inspiratory muscles in rats. J Appl Physiol 1991;70:216–22.
33. Prezant DJ, Aldrich TK, Richner B, et al. Effects of long-term continuous respiratory resistive loading on rat diaphragm function and structure. J Appl Physiol 1993;74:1212–9.
34. Salejee I, Tarasiuk A, Reder I, Scharf SM. Chronic upper airway obstruction produces right but not left ventricular hypertrophy in rats. Am Rev Respir Dis 1993;148:1346–50.
35. Greenberg HE, Tarasiuk A, Rao RS, et al. Effect of chronic resistive loading on ventilatory control in a rat model. Am J Respir Crit Care Med 1995;152:666–76.
36. Tarasiuk A, Segev Y. Chronic resistive airway loading reduces weight due to low serum IGF-1 in rats. Respir Physiol Neurobiol 2005;145:177–82.
37. Everson CA, Crowley WR. Reductions in circulating anabolic hormones induced by sustained sleep deprivation in rats. Am J Physiol Endocrinol Metab 2004;286:E1060–70.
38. Schaub CD, Tankersley C, Schwartz AR, Smith PL, Robotham JL, O'Donnell CP. Effect of sleep/wake state on arterial blood pressure in genetically identical mice. J Appl Physiol 1998;85:366–71.
39. Gradwohl G, Berdugo-Boura N, Segev Y, Tarasiuk A.Chronic upper airway obstruction induces abnormal sleep/wake dynamics in juvenile rats. PLoS One 2014;9:e97111.
40. Bancroft JD, Gamble M, eds. Theory and practice of histological techniques, 6th ed. Philadelphia, PA: Churchill Livingstone, 2008:150.
41. Rosenberg L. Chemical basis for the histological use of safranin O in the study of articular cartilage. J Bone Joint Surg Am 1971;53:69–82.
42. Landau D, Eshet R, Troib A, et al. Increased renal Akt/mTOR and MAPK signaling in type I diabetes in the absence of IGF type 1 receptor activation. Endocrine 2009;36:126–34.
43. Bouxsein ML, Boyd SK, Christiansen BA, Guldberg RE, Japsen KJ, Müller R. Guidelines for assessment of bone microstructure in rodents using micro-computed tomography. J Bone Miner Res 2010;25:1468–86.
44. Pillar G, Shehadeh N. Abdominal fat and sleep apnea: the chicken or the egg? Diabetes Care 2008;31:S303–9.
45. Ben-Israel N, Zigel Y, Tal A, Segev Y, Tarasiuk A. Adenotonsillectomy improves slow-wave activity in children with obstructive sleep apnoea. Eur Respir J 2011;37:1144–50.
46. Tal A. Obstructive sleep apnea syndrome: pathophysiology and clinical characteristics. In: Stephen H, Sheldon DO, Kryger MH, Gozal D, eds. Principles and practice of pediatric sleep medicine. New York, NY: Elsevier, 2014:215–20.
47. Elefteriou F, Takeda S, Ebihara K, et al. Serum leptin level is a regulator of bone mass. Proc Natl Acad Sci U S A 2004;101:3258–63.
48. Ducy P, Amling M, Takeda S, et al. Leptin inhibits bone formation through a hypothalamic relay: a central control of bone mass. Cell 2000;100:197–207.
49. Markwald RR, Melanson EL, Smith MR, et al. Impact of insufficient sleep on total daily energy expenditure, food intake, and weight gain. Proc Natl Acad Sci U S A 2013;110:5695–700.
50. Everson CA, Szabo A. Recurrent restriction of sleep and inadequate recuperation induce both adaptive changes and pathological outcomes. Am J Physiol Regul Integr Comp Physiol 2009;297:R1430–40.
51. Spiegel K, Tasali E, Penev P, Van Cauter E. Brief communication: sleep curtailment in healthy young men is associated with decreased leptin levels, elevated ghrelin levels, and increased hunger and appetite. Ann Intern Med 2004;141:846–50.
52. Martins PJ, Marques MS, Tufik S, D'Almeida V. Orexin activation precedes increased NPY expression, hyperphagia, and metabolic changes in response to sleep deprivation. Am J Physiol Endocrinol Metab 2010;298:E726–34.
53. Tal A, Bar A, Leiberman A, Tarasiuk A Sleep characteristics following adenotonsillectomy in children with obstructive sleep apnea syndrome. Chest 2003;124:948–53.
54. Kezirian EJ, Kirisoglu CE, Riley RW, Chang E, Guilleminault C, Powell NB. Resting energy expenditure in adults with sleep disordered breathing. Arch Otolaryngol Head Neck Surg 2008;134:1270–5.
55. Delhanty PJ, van der Eerden BC, van der Velde M, et al. Ghrelin and unacylated ghrelin stimulate human osteoblast growth via mitogen-activated protein kinase (MAPK)/phosphoinositide 3-kinase (PI3K) pathways in the absence of GHS-R1a. J Endocrinol 2006;188:37–47.
56. Fukushima N, Hanada R, Teranishi H, et al. Ghrelin directly regulates bone formation. J Bone Miner Res 2005;20:790–8.
57. Kim SW, Her SJ, Park SJ, et al. Ghrelin stimulates proliferation and differentiation and inhibits apoptosis in osteoblastic MC3T3-E1 cells. Bone 2005;37:359–69.

58. Caminos JE, Gualillo O, Lago F, et al. The endogenous growth hormone secretagogue (ghrelin) is synthesized and secreted by chondrocytes. Endocrinology 2005;146:1285–92.
59. Nikolopoulos D, Theocharis S, Kouraklis G. Ghrelin, another factor affecting bone metabolism. Med Sci Monit 2010;16:RA147–62.
60. Lecka-Czernik B, Rosen CJ, Kawai M. Skeletal aging and the adipocyte program: new insights from an ''old'' molecule. Cell Cycle 2010;9:3648–54.
61. Wang Y, Sul HS. Pref-1 regulates mesenchymal cell commitment and differentiation through Sox9. Cell Metab 2009;9:287–302.
62. Duque G, Li W, Vidal C, Bermeo S, Rivas D, Henderson J. Pharmacological inhibition of PPARγ increases osteoblastogenesis and bone mass in male C57BL/6 mice. J Bone Miner Res 2013;28:639–48.
63. Hamrick MW, Skedros JG, Pennington C, McNeil PL. Increased osteogenic response to exercise in metaphyseal versus diaphyseal cortical bone. J Musculoskelet Neuronal Interact 2006;6:258–63.
64. Akiyama H, Chaboissier MC, Martin JF, Schedl A, de Crombrugghe B. The transcription factor Sox9 has essential roles in successive steps of the chondrocyte differentiation pathway and is required for expression of Sox5 and Sox6. Genes Dev 2002;16:2813–28.
65. Cheng CC, Uchiyama Y, Hiyama A, Gajghate S, Shapiro IM, Risbud MV. PI3K/AKT regulates aggrecan gene expression by modulating Sox9 expression and activity in nucleus pulposus cells of the intervertebral disc. J Cell Physiol 2009;221:668–76.
66. Henry SP, Liang S, Akdemir KC, de Crombrugghe B. The postnatal role of Sox9 in cartilage. J Bone Miner Res 2012;27:2511–25.
67. Ikegami D, Akiyama H, Suzuki A, et al. Sox9 sustains chondrocyte survival and hypertrophy in part through Pik3ca-Akt pathways. Development. 2011;138:1507–19.

SUBMISSION & CORRESPONDENCE INFORMATION

Submitted for publication October, 2015
Submitted in final revised form December, 2015
Accepted for publication December, 2015
Address correspondence to: Yael Segev, PhD, Department of Microbiology and Immunology, Faculty of Health Sciences, Ben-Gurion University of the Negev, PO Box 105, Beer-Sheva 84105, Israel; Tel: +972-8-647-9898; Fax: +972-8-640-3886; Email: yaelse@bgu.ac.il

DISCLOSURE STATEMENT

This was not an industry supported study. This study was supported by the Israel Science Foundation grant No. 31/14. The authors have indicated no financial conflicts of interest. Dr. Tarasiuk, Avishag Levi, Mohammad Assadi, Ariel Troib and Dr. Segev designed the research. All authors performed the research and analyzed the data. Ariel Tarasiuk and Dr. Segev wrote the manuscript. Drs. Tarasiuk and Segev recruited funds.